



13th International Conference on Greenhouse Gas Control Technologies, GHGT-13, 14-18
November 2016, Lausanne, Switzerland

Synchrotron study of cement hydration: Towards computed tomography analysis of interfacial transition zone

Alexandre Lavrov^{1*}, Elvia Anabela Chavez Panduro², Malin Torsæter¹

¹SINTEF Petroleum Research, Trondheim, Norway

²Department of Physics, Norwegian University of Science and Technology, Høgskoleringen 5, 7491 Trondheim, Norway

Abstract

The quality of bonding between cement and steel in wells is controlled by the interfacial transition zone (ITZ). Micro-computed X-ray tomography (μ -CT) imaging with synchrotron radiation was used in the current paper to study the development of ITZ at the early stages of hydration. The experiments have revealed that the width of the transition zone is around 20 μm , which is consistent with earlier reports. Unlike previously published studies, where the ITZ width was estimated with the naked eye, the ITZ in our study was identified using a quantitative procedure that made use of particle size analysis. This analysis revealed that the ITZ is depleted of large cement particles from the very beginning of hydration.

© 2017 Published by Elsevier Ltd. This is an open access article under the CC BY-NC-ND license (<http://creativecommons.org/licenses/by-nc-nd/4.0/>).

Peer-review under responsibility of the organizing committee of GHGT-13.

Keywords: well cementing; well integrity; cement; hydration; interfacial transition zone (ITZ); cement bonding; debonding; synchrotron; X-ray tomography.

1. Introduction

Integrity of injection wells at CO₂ storage sites is of paramount importance for preventing CO₂ leakage. Potential leakage paths along a cased and cemented well may be due to flaws (cracks, uncemented channels) in cement or due to debonding at cement-casing and/or cement-rock interfaces. Such debonding and flaws can be caused by in-situ stress changes in the reservoir during injection [1,2] or by thermal stresses in the near-well area caused by

* Corresponding author. Tel.: +47 9828-6658
E-mail address: alexander.lavrov@sintef.no

temperature variation during injection [3, 4]. Especially the interfaces between cement and casing (or rock) are vulnerable since previous experiments have shown that fractures often develop in a narrow (tens of μm wide) contact zone near the interface rather than in the bulk cement [5]. This zone, usually called the interfacial transition zone (ITZ), is depleted of large cement grains and is known to have higher porosity and lower strength than the bulk cement [6].

Since ITZ plays a crucial role in debonding and, thus, cement sheath integrity, understanding the structure and formation of ITZ is of paramount importance. In particular, understanding the physical mechanisms behind the ITZ formation is required if we attempt to manipulate the interface to improve its strength.

Up until recently, particle packing disturbances near a solid wall (e.g. casing) caused by geometric constraints were held responsible for the formation of ITZ. Within this view, advocated e.g. in [7], large cement grains cannot pack optimally near a wall. If the near-wall packing configuration were the same as in the bulk cement, some of the large grains would necessarily be cut by the wall.

This line of argument, albeit valid, does not refer to any specific *physical mechanism* that could be responsible for such altered packing in the near-wall region. Two physical mechanisms for disturbed near-wall packing can be thought of:

- 1) large particles cannot grow near the wall during hydration of cement because there is no space;
- 2) large particles cannot approach the wall when cement slurry is poured.

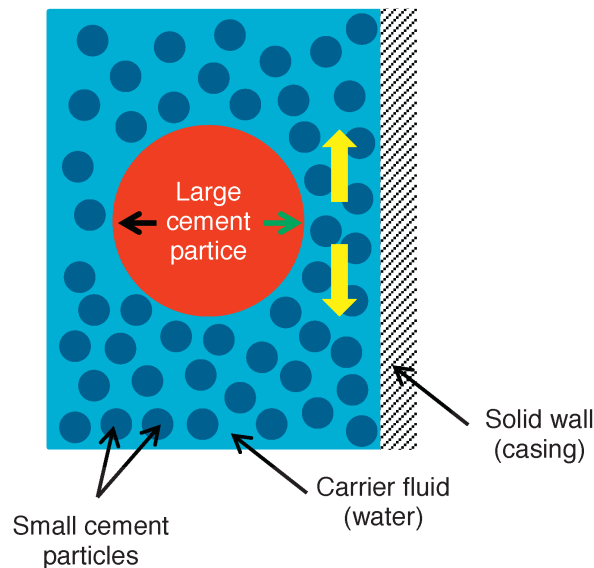


Fig. 1. Large cement particle approaching a solid wall. Particle velocity (green arrow) is directed towards the wall. Lubrication force (black arrow) repels the particle from the wall and thereby slows down particle's approach. Yellow arrows indicate the direction of squeeze flow in the gap between particle and wall.

The first of these explanations implies that disturbed packing develops gradually as hydration proceeds. The second explanation, proposed in [8], stipulates that the near-wall zone is depleted of large cement particles *from the very beginning of hydration*, i.e. when the cement slurry has just been poured. This is due to the lubrication forces acting on large particles: Imagine, for the sake of simplicity, that the cement slurry contains particles of only two sizes, "small" and "large", suspended in the carrier fluid (water). The slurry can then be thought of as a suspension of large particles in a non-Newtonian fluid, this fluid itself being a suspension of small particles in water. When a large particle is moving towards a solid wall, an indirect hydrodynamic force called "lubrication force" acts on the large particle, preventing it from approaching and touching the wall [9-12]. This force is produced because a squeeze flow is generated in the gap between the particle and the wall as the particle approaches (yellow arrows in Fig. 1). In order

to maintain this flow, an increasingly higher pressure gradient is required in the direction of the yellow arrows as the gap closes. Therefore, pressure builds up in the gap, and this pressure pushes the particle back from the wall. The resultant force (black arrow in Fig. 1) applied by the elevated pressure in the gap on the particle surface is the lubrication force. It is this force that prevents large cement particles from approaching the wall.

If the lubrication-based explanation holds, it should be possible to observe the depletion of large particles in the near-wall region from the very beginning of hydration. In order to check this hypothesis, it is necessary to collect high-resolution tomographic images at the early stages of hydration. Such images can be collected e.g. by means of synchrotron X-ray tomography. The synchrotron tomography provides high resolution in both space *and time*, which enables monitoring of cement structure development in real time during hydration.

The objectives of this study were as follows:

- to investigate, to our knowledge for the first time, the development of the interfacial transition zone in cement near a solid wall using high-resolution synchrotron X-ray tomography;
- to find, by analyzing the particle size distributions at different distances from the wall, whether the near-wall zone is depleted of large cement particles *from the very beginning of hydration*.

2. Experiments

Micro-tomographic measurements were carried out at the TOMCAT beamline facility (Swiss Light Source synchrotron at Paul Scherrer Institut in Villigen, Switzerland), using a photon energy of 20 keV. The specimen was prepared by placing Portland G cement paste into a glass tube with the inner diameter of 0.5 mm. Immediately thereafter, the open tube filled with cement was measured over the time in order to study the setting process in-situ. The initial water/cement ratio of the paste was equal to 0.4. This is within the range typical of oil well cements (in field conditions, high water content is intended to improve the pumpability of the slurry). μ -CT scanning was performed 5 min after the cement had been placed in the tube. 1501 projections over 180° have been acquired with an exposure time of 90 ms per projection. The 2D projections were obtained with a field of view of $0.8 \times 0.6 \text{ mm}^2$, a pixel size of $0.33 \times 0.33 \mu\text{m}^2$, and a detector-sample distance of 78 mm. At this distance the absorption contrast is enhanced because of the phase contrast. For the reconstruction of the absorption-contrast 2D projections, the ANKAphase software was used [13]. An image of the tube's cross section is shown in Fig. 2. The near-wall zone of disturbed packing is visible in Fig. 2.

Image visualization and analyses were carried out using the VGstudio software.. The calculations of the particle volume, particle surface and minimum distance from particle's surface to wall were done in a 3D filtered volume over 253 slices.

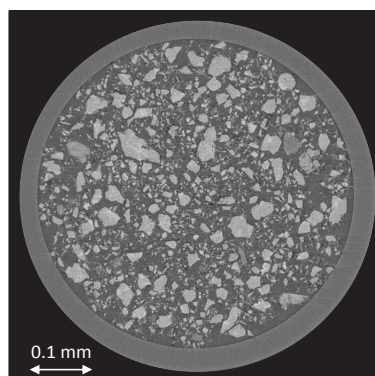


Fig. 2. μ -CT_image_collected at 5 min after cement placement in the tube. The inner diameter of the tube is 0.5 mm.

3. Particle size distribution in the near-wall zone

Since our goal in this study was to investigate what is happening in cement near the wall at the very beginning of hydration, only the first scan (the one collected after 5 min of hydration) was analyzed for the particle size distribution. For each particle in the scan, the following parameters were obtained from the μ -CT images:

- Cartesian coordinates of particle's centroid;
- particle volume;
- particle surface area;
- minimum distance from particle's surface to wall (this parameter is simply called "distance to wall" in the remainder of the paper).

We need to discriminate between "large" and "small" particles in our analyses. Since the shape of cement particles is rarely spherical, an equivalent particle size must be defined, to begin with. There are a number of ways to define the equivalent diameter. In particular, the equivalent size of an irregularly-shaped particle can be defined as the diameter of a spherical particle having the same volume as that of the irregularly-shape particle [15]. This method was employed in our analyses.

In order to quantify the particle size distribution and its variation with distance to wall, two methods were designed and applied to the first μ -CT scan (the scan collected after 5 min of hydration). In the first method (Method A), the relative number of "large" particles was evaluated in two layers, first layer being next to wall and second layer being next to the first layer (Fig. 3). In the second method (Method B), the equivalent particle size was plotted versus particle's distance to wall.

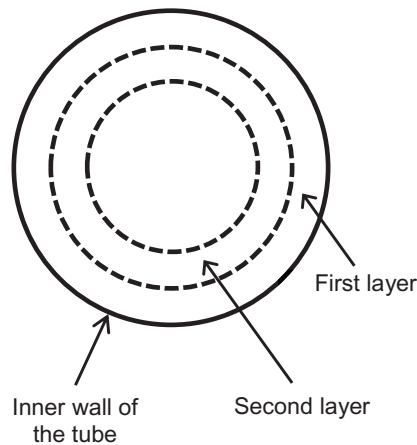


Fig. 3. Two layers in which large and small particles were counted. Not to scale.

3.1. Method A: relative number density of "large" particles

In this method, we first discriminate between "large particles" and "small particles". To this end, a discrimination threshold needs to be assigned for the particle volume. In this study, two analyses were performed, with the discrimination level chosen as two times or one time the average particle volume in the sample. Particles having the volume above this discrimination threshold were labelled "large". Particles below the discrimination threshold were labelled "small".

As explained earlier in this text, our goal was to confirm that there exists a zone depleted of large particles, and to find the width of this zone (its extent from the wall). In order to do the latter, the procedure described below was applied under the assumption of different ITZ sizes. Thus, in each of the two analyses mentioned above, the assumed ITZ width was consecutively assigned different values, from 10 to 100 μm . For each of the assumed ITZ width values, the following procedure was applied:

- Establish two layers in the tube, the first layer being next to wall, the second layer being next to the first layer. The layers have the same width, equal to the assumed ITZ width.
- Count large and small particles in each of the two layers. A particle is deemed to be located in the layer if its centroid is within the layer.
- Calculate the ratio of the large-particle number to the small-particle number for the first layer (next to wall), n_1 , and for the second layer (second next to wall), n_2 .
- Calculate the ratio of the two numbers, $N = n_1/n_2$.

If the assumed ITZ width is equal to the true ITZ width in the sample, N must be quite low. When the assumed ITZ width increases above the true ITZ width, N is expected to increase as well. When the assumed ITZ width becomes much larger than the true ITZ width, N must become insensitive to the assumed ITZ width since now both layers represent bulk cement, with approximately the same proportions of small and large particles. The value of N must therefore asymptotically approach 1 as the assumed ITZ width increases.

The above procedure was repeated for all assumed ITZ width values, from 10 to 100 μm , and the value of N was then plotted as a function of the assumed ITZ width. The resulting plots are shown in Fig. 4 for the discrimination threshold values equal to 2 and 1 times the average particle volume. In both plots in Fig. 4, the value of N starts increasing rapidly once the assumed ITZ width exceeds 20 μm . Thus, based on Method A, the width of the ITZ in this experiment is 20 μm .

Oscillations around $N = 1$ visible in both plots in Fig. 4 are similar to those reported by Suzuki et al. in their experiments in particle packing [16].

One of the weaknesses of Method A is that it might undersample large particles in the near-wall layer. Indeed, in this Method, a particle is deemed to lie in a layer if its *centroid* is in the layer. Thus, a very large particle could almost touch the wall, but still be counted in layer 2 because its centroid is far away from the wall. This drawback of Method A motivated us to apply another, different method to particle size analyses (Subsection 3.2).

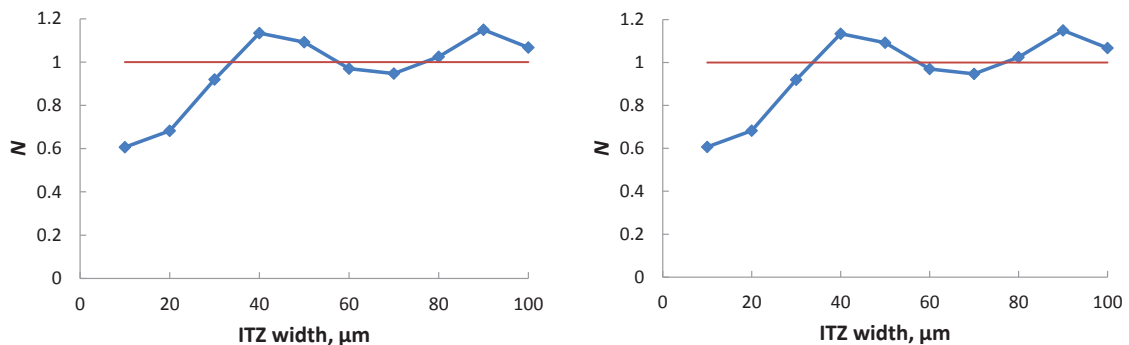


Fig. 4. The value of N (see bulk text for definition) as a function of the assumed ITZ width assuming the discrimination level between large and small particles being two times the average particle volume in the sample (left-hand panel) and being equal to the average particle volume in the sample (right-hand panel). Red lines indicate the asymptotic value of $N = 1$ for large values of the assumed ITZ width.

3.2. Method B: particle size vs. distance to wall

In this method, we plot the equivalent particle size as a function of distance to wall. Distance to wall is defined as the gap between the particle and the wall. Thus, the location of particle's centroid does not matter in this Method. The result is presented in Fig. 5. The ITZ in Fig. 5 is approximately 10 μm wide and appears as the near-wall zone depleted of large particles. In order to confirm these observations quantitatively, the following data processing procedure was employed: Five-micron wide layers were created at different distances from the wall, up to 100 μm into the cement. For each layer, the number of large particles and the number of small particles having distance to wall within that layer were calculated. The ratio of these two numbers was then plotted as a function of the layer distance from the wall (the first layer, located from 0 to 5 μm from the wall, had the distance of 2.5 μm , the second layer had the distance of 7.5 μm , etc.). This analysis was repeated for two discrimination levels between large and small particles: 20 μm and 35 μm . The results are presented in Figs. 6a and 6b, respectively. The results obtained with the two different discrimination levels are consistent with each other and suggest the ITZ width of 15 to 20 μm . The results of Method B are thus consistent with Method A.

Hence, it can be concluded that *the near-wall region, commonly known as the ITZ, is indeed depleted of large particles from the very beginning of hydration. The width of the zone depleted of large particles (the ITZ) is approximately 20 μm .*

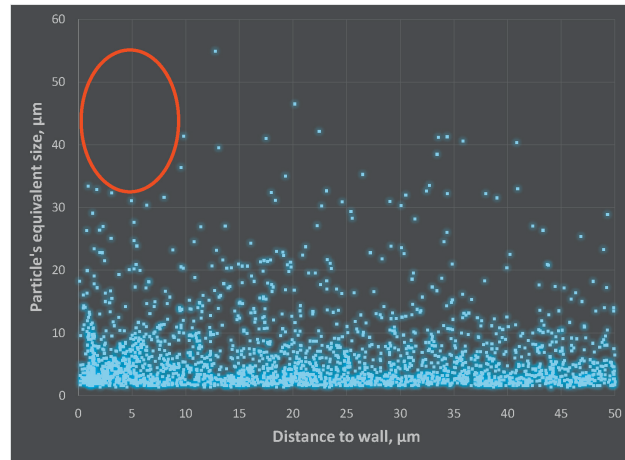
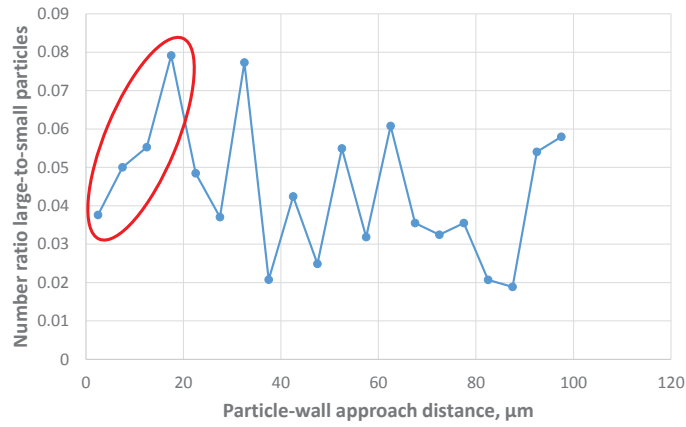
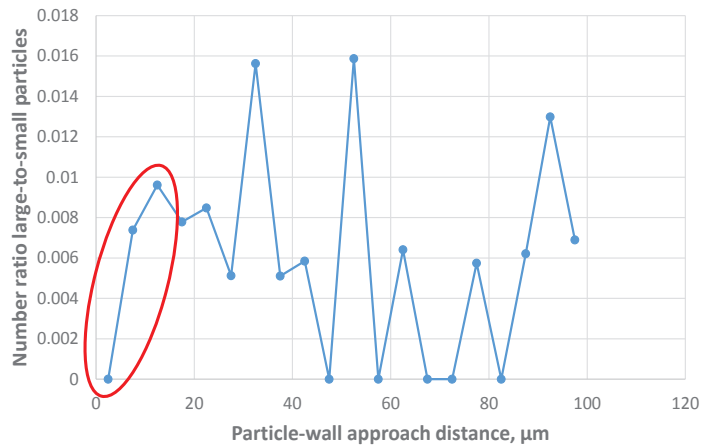


Fig. 5. Particle's equivalent size as a function of distance to wall (minimum distance between the particle surface and the wall). The 10- μm zone depleted of large particles is highlighted.



a



b

Fig. 6. Ratio of large-particle number to small-particle number as a function of the particle-wall approach distance. Discrimination between large and small particles is based on their equivalent size. The discrimination level is equal to 20 μm (a) and 35 μm (b). Region depleted of large particles is highlighted.

4. Discussion

Experiments described in this paper confirm that it is possible to use high-resolution μ-CT imaging to study the development of the interfacial transition zone during hydration. Moreover, we have established image analysis procedures that enable us to evaluate the width of ITZ and the particle size distribution within the ITZ and compare the latter to the bulk cement. Such procedures are needed when developing new cements and other sealant materials since they provide an objective, quantitative description of the interface structure. Given two types of cement, X and Y, a plot similar to Fig. 6 could be used to characterize the extent of structural disturbances in cement near the wall.

A cement having a flat horizontal curve near the wall would indicate that the cement structure is the same near the wall as in the bulk far away from the wall.

The size of the ITZ obtained in this study (20 μm) is consistent with earlier reported values of 10 to 50 μm . In those studies, the ITZ width was estimated visually from the images [8] or was inferred from the measurements of mechanical properties of cement at different distances from the wall using e.g. micro- or nanoindentation techniques [6]. In this study, we have confirmed the earlier visual observation using a quantitative analysis of particle size distribution in different regions of the sample.

The wall in our experiments was made of glass, a dielectric material. In well construction, the wall is either the casing or the rock. Casing, made of (conductive) steel, has different electric properties than glass. This may affect its interaction with cement since cement slurry usually contains charged particles [17, 18]. Electric properties of the wall might therefore influence the size and structure of the ITZ. The experimental procedures used in this study (μ -CT imaging) may be less suitable when the tube is made of steel or other materials poorly transparent to X-rays. The data processing techniques described in Section 3 are free of any limitations and can be used whenever high-quality images are available, with the resolution sufficient for measuring particle sizes and positions.

Additional experiments with the same or different tube diameter should be carried out in future to improve statistics and to study the effect of the surface curvature on the ITZ structure in cement.

Our results are different from earlier reports on particle packing near the wall without interstitial fluid [16]. In those studies, it was found that large particles make a regular arrangement near a wall, which increases the void fraction between large particles. In our study, large particles do not approach the wall. This is apparently due to the interstitial fluid present between the particles. The lubrication force due to this fluid prevents large particles from approaching the wall altogether.

5. Conclusion

High-resolution μ -CT imaging makes it possible to study the interfacial transition zone near a cement-wall interface at the early stages of hydration. The experiments on hydration of neat cement in a glass tube have revealed that the width of the transition zone is around 20 μm . This value is consistent with earlier reports. Unlike earlier studies, where the width was typically estimated with the naked eye, our estimates of the ITZ width are based on a well-defined quantitative procedure involving particle size analysis. This analysis has also revealed that the transition zone is depleted of large cement particles from the very beginning of hydration. This supports an earlier conjecture that large particles cannot approach the wall during cement slurry placement, which is most likely due to the lubrication force slowing down large particles as they move towards the wall.

The imaging procedures and particle size analysis algorithms developed in this study can be used for discriminating between different well sealants with regard to their ability to preserve structure near a solid wall.

Acknowledgement

The authors gratefully acknowledge Dag Breiby (Norwegian University of Science and Technology) whose comments helped to improve the quality of the manuscript. This publication has been produced in the project "Closing the gaps in CO₂ well plugging" funded by the Research Council of Norway (243765/E20). The project is administered as an integrated part of the BIGCCS Centre funded by Gassco, Shell, Statoil, Total, Engie and the Research Council of Norway (193816/S60). We thank Anne Bonnin for her assistance with the μ -CT measurements at the beamline TOMCAT at the Swiss Light Source.

References

- [1] Lavrov A Dynamics of Stresses and Fractures in Reservoir and Cap Rock under Production and Injection. *Energy Procedia* 2016; 86: 381-90.
- [2] Holt RM, Gheibi S, Lavrov A Where does the stress path lead? Irreversibility and hysteresis in reservoir geomechanics. Paper ARMA 16-496 presented at the 50th US Rock Mechanics / Geomechanics Symposium held in Houston, Texas, USA, 26-29 June 2016. 2016.
- [3] Lavrov A, Cerasi P. Numerical modeling of tensile thermal stresses in rock around a cased well caused by injection of a cold fluid. ARMA paper 13-306 present at the 47th US Rock Mechanics / Geomechanics Symposium held in San Francisco, CA, USA, 23-26 June 2013. In: . 2013.
- [4] Lavrov A, Tors ater M. *Physics and Mechanics of Primary Well Cementing*. Springer; 2016.
- [5] Bentur A, Diamond S, Mindess S The microstructure of the steel fibre-cement interface. *Journal of Materials Science* 1985; 20: 3610-20.
- [6] Zhu W, Bartos PJM Application of depth-sensing microindentation testing to study of interfacial transition zone in reinforced concrete. *Cement and Concrete Research* 2000; 30: 1299-304.
- [7] Scrivener K, Crumbie A, Laugesen P The Interfacial Transition Zone (ITZ) Between Cement Paste and Aggregate in Concrete. *Interface Science* 2004; 12: 411-21.
- [8] Tors ater M, Todorovic J, Lavrov A Structure and debonding at cement–steel and cement–rock interfaces: Effect of geometry and materials. *Construction and Building Materials* 2015; 96: 164-71.
- [9] Joseph GG, Zenit R, Hunt ML, Rosenwinkel AM Particle–wall collisions in a viscous fluid. *Journal of Fluid Mechanics* 2001; 433: 329-46.
- [10] Kim S, Karrila SJ. *Microhydrodynamics: principles and selected applications*. Mineola: Dover Publications; 2005.
- [11] Lavrov A, Laux H. DEM modeling of particle restitution coefficient vs Stokes number: The role of lubrication force. Paper No S2_Thu_C_54. In: 6th International Conference on Multiphase Flow, ICMF 2007, Leipzig, Germany, July 9 – 13, 2007. 2007.
- [12] Xu C, Yuan L, Xu Y, Hang W Squeeze flow of interstitial Herschel–Bulkley fluid between two rigid spheres. *Particuology* 2010; 8: 360-4.
- [13] Weitkamp T, Haas D, Wegrzynek D, Rack A ANKAphase: software for single-distance phase retrieval from inline X-ray phase-contrast radiographs. *J. Synchrotron Radiat* 2011; 18: 617-29.
- [14] Schneider CA, Rasband WS, Eliceiri KW NIH Image to ImageJ: 25 years of image analysis. *Nature Methods* 2012; 9: 671-5.
- [15] Shook CA, Roco MC. *Slurry flow: principles and practice*. Stoneham: Butterworth-Heinemann; 1991.
- [16] Suzuki M, Shinmura T, Iimura K, Hirota M Study of the Wall Effect on Particle Packing Structure Using X-ray Micro Computed Tomography. *Advanced Powder Technology* 2008; 19: 183-95.
- [17] Nachbaur L, Mutin JC, Nonat A, Choplin L Dynamic mode rheology of cement and tricalcium silicate pastes from mixing to setting. *Cement and Concrete Research* 2001; 31: 183-92.
- [18] Lavrov A, Gawel K, Tors ater M Manipulating cement-steel interface by means of electric field: Experiment and potential applications. *AIMS Materials Science* 2016; 3: 1199-207.